Effect of Peach Palm Fiber Microstructure on its Tensile Behavior

Juan Pablo Villate Diaz,[a] Flávio de Andrade Silva,[a]* and José Roberto Moraes d'Almeida [b]

This paper presents the results of an experimental investigation into the mechanical behavior and microstructural characteristics of peach palm fibers. The fiber morphology was studied using a scanning electron microscope (SEM), and the results of the mechanical tests were correlated with the fiber microstructure. The specimens were submitted to direct tensile tests in a state-of-the art microforce testing system using three different gauge lengths. The cross sectional areas of the fibers were measured using SEM micrographs and image analysis. The fiber microstructural characteristics were determined *via* thermogravimetric analysis and X-ray diffraction. The measured Young's modulus was corrected for machine compliance. Weibull statistics were used to quantify the degree of variability in fiber strength at the different gauge lengths. The failure mechanisms were described and discussed in terms of the fiber microstructure, as well as defects in the fiber. The results showed that the fiber void content had a large influence on the fiber tensile strength and elastic modulus but the amount of main voids did not influence the fiber strength.

INTRODUCTION

Conventional construction materials such as concrete and steel are the most important components in infrastructure. The elevated cost of these materials and the negative impact on the environment has increased the use of natural materials (George *et al.* 2001). In recent years, non-conventional materials, such as cement and polymer matrix composites reinforced with vegetable fibers, have become attractive alternatives (Hota and Liang 2011). Composites reinforced with vegetable fibers can reduce the waste from construction, increase the energy efficiency of infrastructure, and promote the concept of sustainability (Dittenber and GangaRao 2012).

Vegetable fibers have important advantages, such as their low cost compared with other conventional reinforcements, low density, high mechanical properties, and adequate thermal and acoustic insulation properties. Vegetable fibers are a renewable source and available anywhere in the world, and therefore, accessible for people with low incomes living in poor regions (Gaceva 2007). Vegetable fibers can be used in several areas, such as reinforcement of polymer-based composites for vehicles, textiles, and reinforcement in cementitious composites. Each fiber has different and unique properties depending on certain factors, such as fiber diameter, microstructure, degree of crystallinity, method of extraction, and the conditions of the plant before harvest (Marinelli *et al.* 2008).

Several studies have been performed to determine the mechanical behavior of vegetable fibers (De Rosa *et al.* 2011; Bezazi *et al.* 2014; Belouadah *et al.* 2015; Porras *et al.* 2015). These studies show that the tensile strength depends on the proportion of cellulose, degree of crystallinity, fiber morphology, microfibrilar angle, test methods, and plant characteristics, as reported for piassava (d'Almeida *et al.* 2006), coir (Defoirdt *et al.* 2010; Ferreira *et al.* 2014), jute (Fidelis *et al.* 2013), sisal (Silva *et al.* 2008), bamboo (Prasad and Rao 2011), flax (Baley 2002), okra (De Rosa *et al.* 2010), kenaf (Akil *et al.* 2011), *Lygeum spartum* L. (Belouadah *et al.* 2015), banana (Prasad and Rao 2011), curauá (Tomczak *et al.* 2007; Spinacé *et al.* 2009), alpha (Brahim and Cheikh 2007), hemp (Jayaramudu *et al.* 2010) and areca (Srinivasa *et al.* 2011; Chakrabarty *et al.* 2012; Padmaraj *et al.* 2013; Yusriah *et al.* 2014; Binoj *et al.* 2016). The mechanical behaviors of these fibers are classified depending on their tensile strength and modulus of elasticity. Among the low tensile strength category are piassava (143 to 175 MPa), alpha (152 to 210 MPa), *Lygeum* (75 to 225 MPa), coir (175 to 245 MPa), okra (195 to 235 MPa), and areca (123 to 322 MPa). Jute fibers have moderate tensile strength (299 to 450 MPa). Sisal (375 to 577 MPa), hemp (388 to 570 MPa), banana (565 to 725 MPa), curauá (700 to 900 MPa), and bamboo (710 to 915 MPa) are classified as high strength fibers. The high variability of the results can be traced back to the testing procedure, the methodology used for calculating the fiber cross sectional area, the plant age, harvest location, fiber humidity, and machine compliance.

The crystallinity index (CI) of natural fibers ranges from 40% to 70%, as reported for coconut fibers (41.9%) (Carvalho *et al.* 2010), *Lygeum spartum* L. (47%) (Belouadah *et al.* 2015), *Sansevieria ehrenbergii* (52.27%) (Sreenivasan *et al.* 2011), and *A. officinalis* L. (70%) (Sarikanat *et al.* 2014). The thermal decomposition of the main components of natural fibers occurs at different temperatures. Lignin, hemicellulose, and cellulose decompose between 280 and 500 °C, 200 and 500 °C, and 240 and 350 °C, respectively (Seki *et al.* 2013). Thus, natural fibers are thermally stable from about 200 to 275 °C (Fiore *et al.* 2014; Sarikanat *et al.* 2014; Belouadah *et al.* 2015).

A previous study on the tensile behavior of natural peach palm fiber suggested that to understand the variability of their tensile properties, a deep microstructural analysis should be performed. The correct understanding of its mechanical behavior and microstructural characteristics is desirable to determine possible future applications, such as reinforcement in cementitious and polymeric matrices (Temer and d'Almeida 2012).

This work presents mechanical and microstructural tests carried out on natural peach palm fibers. The mechanical results were correlated with the fiber microstructure. This correlation was made by observing fibers in the scanning electron microscope (SEM) to determine their cross sectional area and then performing direct tensile tests on the same specimens. The three areas studied were the total area, the area without the main voids, and the effective area. The microstructural properties of the fibers were determined by thermogravimetric analysis (TGA) and X-ray diffraction (XRD).

EXPERIMENTAL

Fiber Extraction

The peach palm fibers used in this paper were extracted from the trunk of the palm by a manual process. The palm plant was located in Buenaventura, Colombia in the Valle de Cauca department. The extraction of the fiber was performed in four steps. First,

the trunk was cut into four sections. With a rubber hammer, the trunk was crushed to soften the structure in order to facilitate the fiber extraction process. After adding water, the fibers were manually extracted with tweezers. Finally, the fibers were treated with hot water (~40 °C) to eliminate surface impurities. In the present paper the term "fiber" will refer to a multi-cellular composite structure, which is the case for the peach palm fiber. The term "fiber-cell" is used in reference a single unit cellular structure.

Fiber Morphological Analysis

The fiber microstructure, before and after tensile fracture, was analyzed using a JEOL JSM-6510 LV SEM (JEOL, Tokyo, Japan). The electron microscope was operated in the secondary electron mode under 20 kV accelerating voltage and a working distance ranging from 8 to 10 mm. The fibers were pre-coated with a thin layer of gold.

To measure the cross sectional area for each tested fiber under tensile load, an adjacent piece of the fiber (immediately next to the one tested) was kept for future measurement using the SEM.

The morphological analysis was carried out to determine three different types of areas, which were *At* (the total area, Fig. 1a), *Ad* (the area without the main voids, Fig. 1b), and *Ae* (the effective area without any void, Fig. 1c). This was done to evaluate the influence of porosity on the fiber mechanical behavior. The images were post-processed using the software ImageJ (National Institutes of Health, Bethesda, MD, USA), a Java-based image processing program.

X-Ray Diffraction

To determine the CI of the peach palm fiber and to evaluate its content of cellulose, XRD tests were carried out. The tests were performed on a D8 DISCOVER diffractometer system (Bruker, Billerica, U.S.A.). The copper radiation was Cu-Kα, $\lambda =$ 1.5406 Å, and the equipment was operated at 40 kv and 30 mA. The specimens were analyzed between Bragg angles (2θ) of 5° to 70° with 0.02° angular speed per s. to determine the amount of crystallinity, the deconvolution method of crystalline peaks and amorphous halo was used. For this process, the Origin 9.0 software (OriginLab Corp., Northampton, U.S.A.) with a Gaussian function was used.

The diffractogram was separated into various components that independently contributed to the formation of the peaks in each phase. The quantitative decomposition of XRD provided a measure of CI using Eq. 1,

$$CI = \frac{Ac}{Ac + Aa}100\%$$ (1)

where *CI* is the crystallinity index of the material, *Ac* is the area below the crystalline peaks (a.u. *versus* degrees), and *Aa* corresponds to the area of amorphous halo (a.u. *versus* degrees).

Thermogravimetric Analysis (TGA)

The tests were performed in a Simultaneous Thermal Analyzer (STA) 6000 (PerkinElmer, Waltham, USA). A knife mill was used to produce 8 mg powder fiber samples. The fibers were subjected to a heating rate of 10 °C/min until reaching 800 °C, in an open platinum pan with nitrogen as the purge gas, which had a flow rate of 20 mL/min.
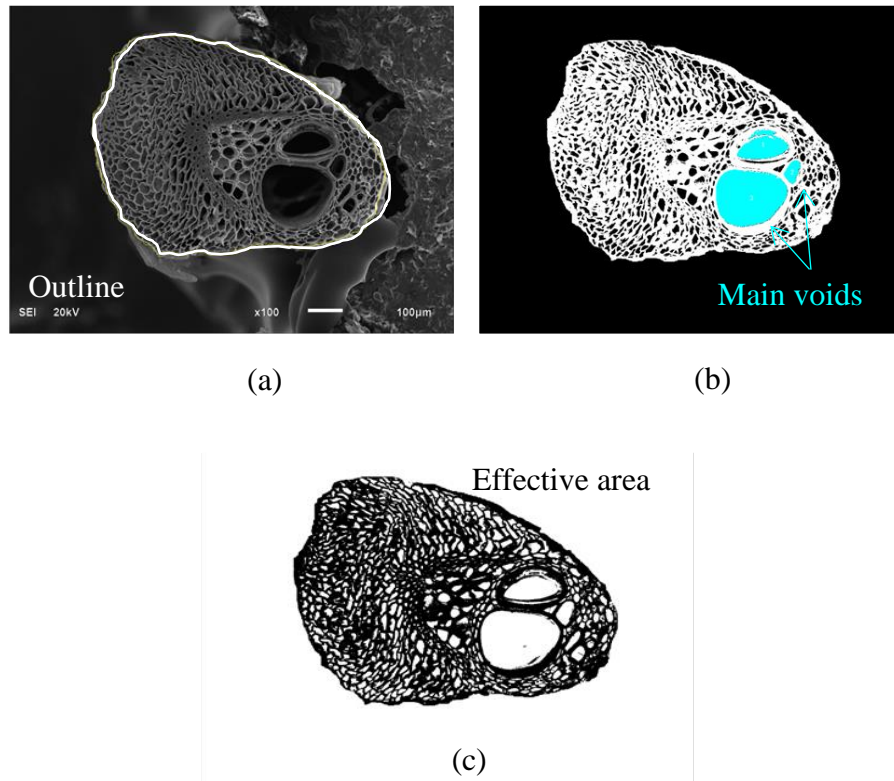
Fig. 1. The fiber cross sectional area computation using the SEM micrographs in ImageJ software: (a) total area determination, (b) analysis of the area without the main voids which are used for the transport of the sap, and (c) analysis of the area without all voids (the effective area)

Direct Tensile Behavior

The fibers, tested in their dry natural state, were submitted to tensile loading for three different gauge lengths (GL), which were 20, 30, and 40 mm. The tests were performed in a MTS Tytron 250 (MTS Systems, Minneapolis, MN, USA) (Fig. 2). The tested fibers were arranged according to ASTM C1557 (2014). Tensile tests were performed with a displacement control rate of 0.1 mm/min and a load cell of 50 N. All tests were performed at room temperature (~22 °C) with relative humidity at approximately 60%.

The compliance of the frame and gripping system was obtained by determining the force *versus* displacement of the fiber for three different gauge lengths, following the methodology described elsewhere (Silva *et al.* 2008). The total displacement of the system during the tensile tests in the fiber, δ_t (mm), was determined by Eq. 2,

$$\frac{\delta_t}{F} = \left[\frac{1}{EA}\right] l + c \qquad (2)$$

where c is the machine compliance, F is the applied force (N), E is the Young's modulus of the fiber (MPa), A is the cross-sectional area of the fiber (mm^2), and l is gauge length (mm). A plot of δ_t / F *versus* l yielded a straight line with slope $1 / (EA)$ and intercept c.

Fig. 2. The direct tensile test setup of the MTS Tytron 250 and a zoom in showing the load cell and the peach palm fiber specimen

RESULTS AND DISCUSSION

Fiber Morphology

The peach palm fiber had a structure in which each fiber had numerous individual fiber cells along the length. The fiber cells were composed of four main parts, which were the primary wall, the secondary wall, the tertiary wall, and the lumen (Fig. 3). The fiber cells were joined together by means of hemicellulose and lignin, and they are called the middle lamella (ML) (Fig. 3b, 3c). This type of structure is similar to those observed for other vegetable fibers (Silva *et al.* 2008).
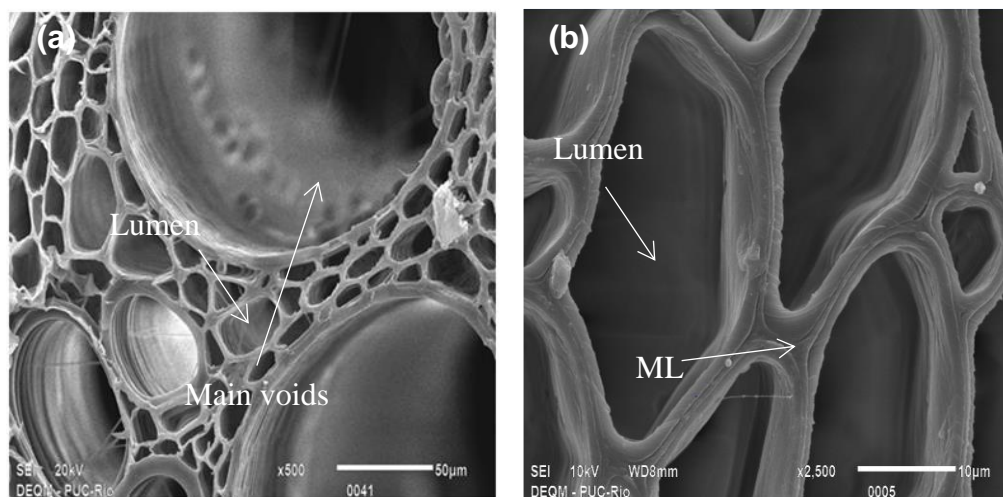
Fig. 3 (a & b). Peach palm fiber microstructure: (a) fiber cells and main voids with its lumen, (b) detail of the fiber cells with the middle lamella between them
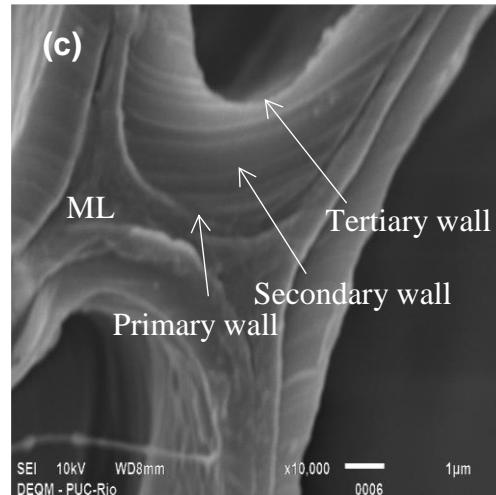
Fig. 3 (c). The peach palm fiber microstructure: (c) detail of the walls of the fiber cells

The morphology of the peach palm fiber differed in the amount of main voids (or main lumens) that are used to transport the cell sap, *i.e*., watery fluid that circulates through the plant and carries food and other substances to various tissues (Fig. 3a, Fig. 4). In this work, we observed peach palm fibers with the number of main voids ranging from 1 to 4 (Fig. 4). The measurements of the three different areas resulted in values of 0.39 to 0.41 mm^2 for *At*, 0.35 to 0.37 mm^2 for *Ad*, and 0.26 to 0.28 mm^2 for *Ae* (Table 1.).

(a)

(b)

(c)

(d)
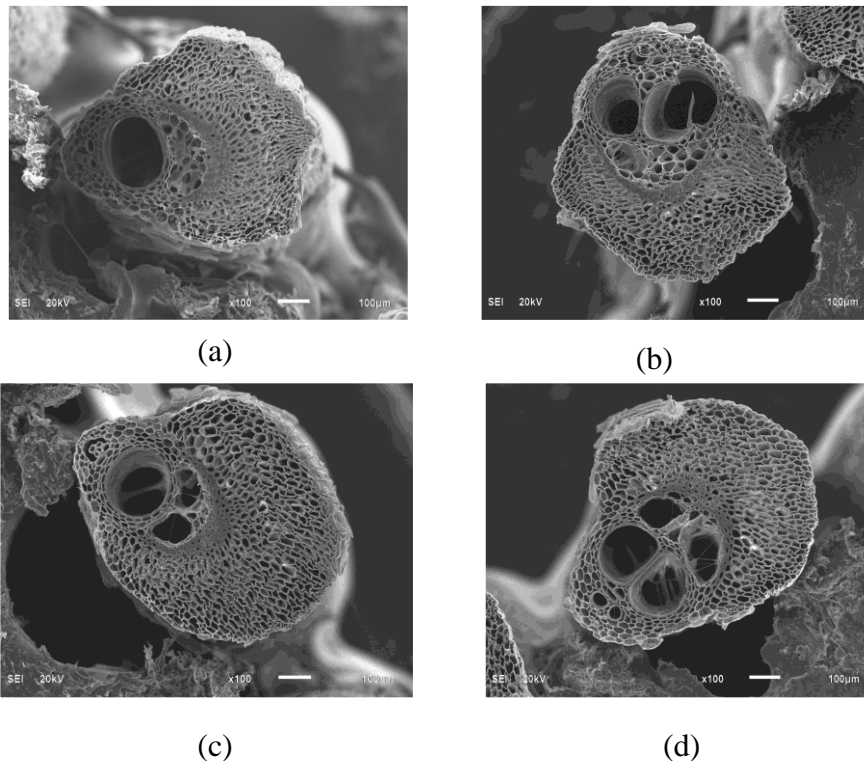
Fig. 4. Morphologies of the peach palm fibers according to the number of main voids: (a) one void, (b) two voids, (c) three voids, and (d) four voids

The microstructural observation performed in the peach palm fibers showed that the quantity of main voids was not a function of the total area of the fiber (Fig. 5a). The diameter of the main voids tended to increase when the number of main voids increased (Fig. 5b).

(a)   (b)
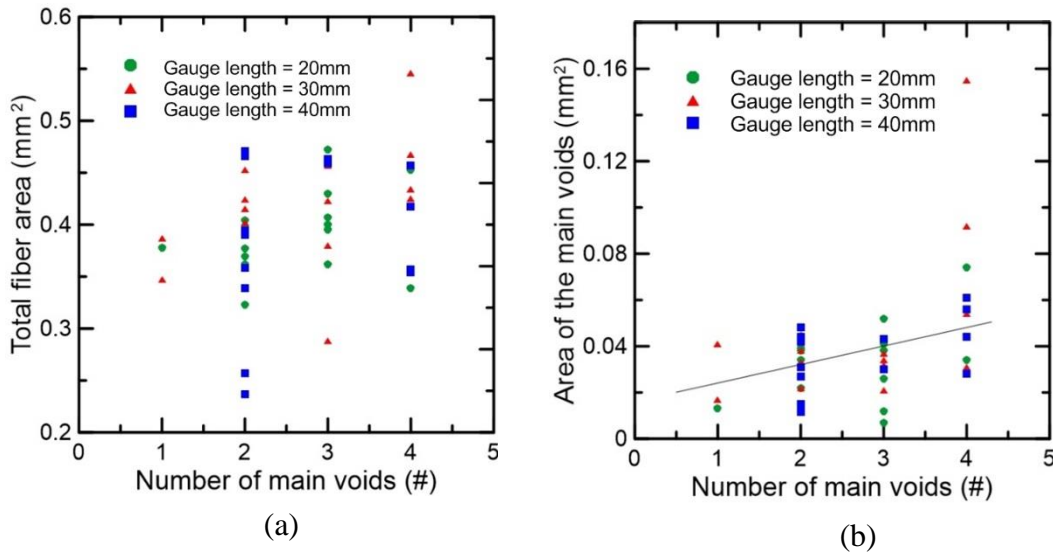
Fig. 5. The effect of the main voids on the fiber area: (a) number of the main voids *versus* total fiber area and (b) number of main voids *versus* area of main voids

The cross sectional area calculation for peach palm fibers, as well as for other vegetable fibers, can result in considerable errors if a circular shape form is adopted. Therefore, the cross sectional area and porosity should be taken into account when computing the fiber tensile stress.

X-Ray Diffraction and TGA Analysis

The diffraction spectrum of X-rays had three characteristic peaks for the peach fibers and an amorphous halo.

(a)   (b)
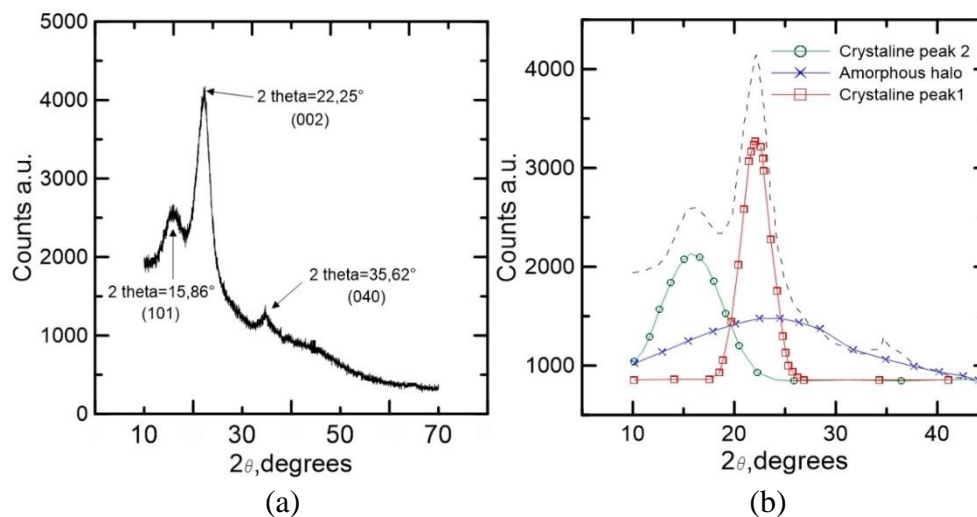
Fig. 6. (a) X-ray analysis of peach palm fiber and (b) analysis carried out in the Origin 9.0 software to determine the CI

bioresources.com

The peak with the highest intensity at $2\theta = 22.25°$ corresponded to the (002) plane; the average intensity peak at $2\theta = 15.86°$ corresponded to the (101) plane. The angle $2\theta = 35.62°$ was a peak of low intensity that corresponded to the (040) plane. These results were similar to cellulose in other natural fibers (Rong *et al.* 2001; d'Almeida *et al.* 2006, 2008) (Fig. 6a).

The analysis of deconvolution of the crystalline peaks and amorphous halo was carried out in the range of 10° to 45° using the Origin 9.0 software Gaussian function, with a correlation factor (R^2) of 0.993 (Fig. 6b). Only the two highest peaks were included in the deconvolution analysis. The third peak, at $2\theta = 35.62°$, was not included because of its very low intensity. The CI, calculated according to Eq. 1, was 61%.
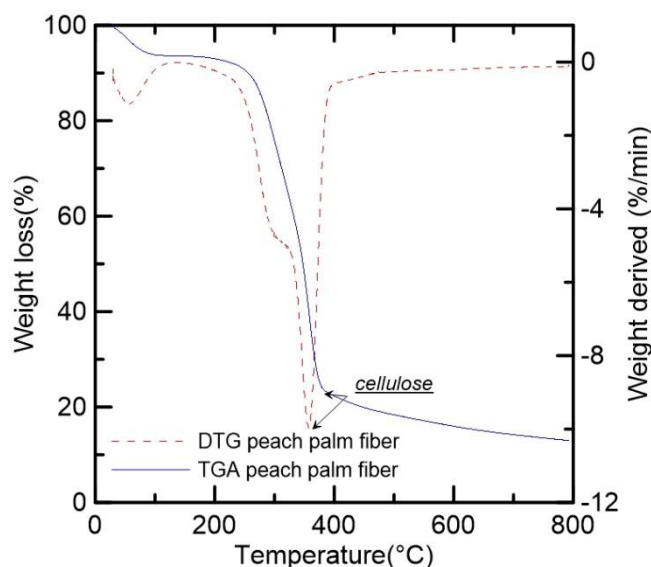
Fig. 7. TGA of the peach palm fiber

Figure 7 shows the TGA of the peach palm fiber. Three events of mass loss occurred. Initially, a decrease in humidity caused a weight loss of 9% at temperatures ranging from 50 to 100 °C.

Subsequently, the decomposition of hemicellulose began, which caused weight loss at approximately 300 °C. Finally, the degradation phase, which is linked with the fiber thermal decomposition of cellulose, occurred at 367 °C (Fig. 7). The results showed that the peach palm fiber was thermally stable up to 280 °C, which was similar to other natural fibers (d'Almeida *et al.* 2006; De Souza and d'Almeida 2014; Belouadah *et al.* 2015; Porras *et al.* 2015).

Fiber Mechanical Behavior

A total of 15 fibers were randomly chosen from a batch to perform the tensile tests, and each gauge length was tested. To calculate the Young's modulus of the peach palm fiber, it was first necessary to correct the flexibility in the machine's ability to calculate the elastic region of the stress-strain curve according to Eq. 5 (Fig. 8a).

The variability of the corrected and uncorrected Young's modulus did not present much difference. This demonstrated that the machine that was used had a high stiffness (Fig. 8b).

bioresources.com

(a)

(b)

(c)
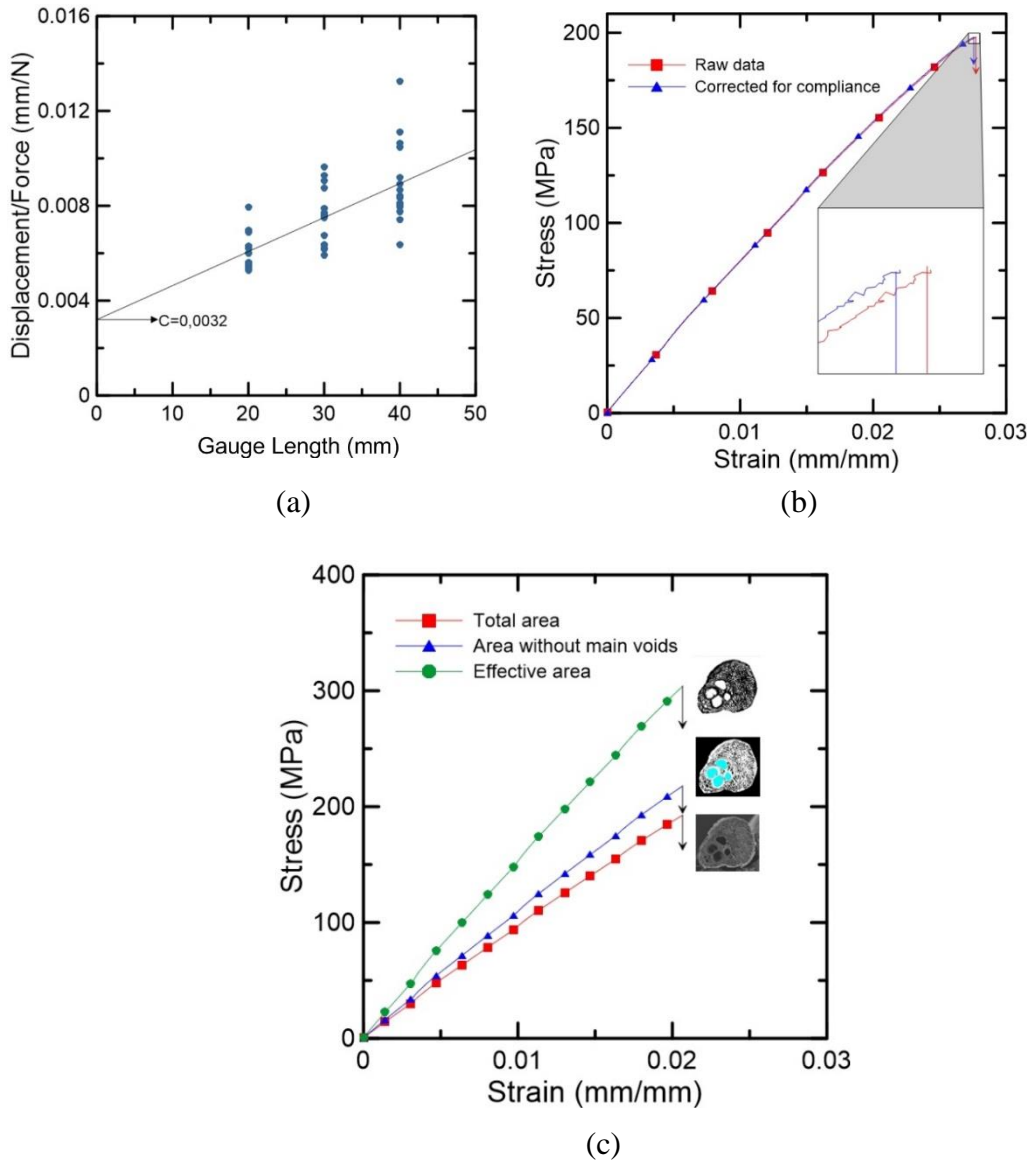
Fig. 8. The direct tensile behavior of the peach palm fiber: (a) displacement/force *versus* gauge length of the peach palm fiber to determine the machine flexibility, *c*, (b) stress *versus* strain curve corrected for the machine compliance, and (c) influence of area (total area, area without main voids, and the effective area) on the stress *versus* strain behavior of the peach palm fiber

The peach palm fiber had an average tensile strength of 213.5 MPa and a Young's modulus of 10.8 GPa when the total area was used (area taking into account all voids). This behavior was compared to that of other natural fibers, such as piassava (d'Almeida *et al.* 2006), coir (Defoirdt *et al.* 2010; Ferreira *et al.* 2014), jute (Fidelis *et al.* 2013), sisal (Silva *et al.* 2008), curauá (Tomczak *et al.* 2007; Spinacé *et al.* 2009), bamboo (Prasad and Rao 2011), okra (De Rosa *et al.* 2010), *Lygeum spartum* L. (Belouadah *et al.* 2015), banana (Prasad and Rao 2011), alpha (Brahim and Cheikh 2007), and hemp (Jayaramudu *et al.* 2010).

The tensile stress was also computed as a function of the fibers microstructure. The fiber strength increased considerably when the effective area was taken into account (Fig. 8c, Table 1).

Table 1. Average Results and Standard Deviation of the Tensile Tests Carried on Peach Palm Fibers

Area Type	Gauge Length (mm)	Area (mm^2)		Tensile Strength (MPa)		Strain-to-Failure (%)		As-measured Young's Modulus (GPa)		Weibull Modulus
At	20	0.39	± 0.04	196.2	± 17.8	2.7	± 0.26	7.7	± 0.8	12.9
	30	0.41	± 0.06	198.5	± 19.7	2.2	± 0.30	9.5	± 1.2	11.9
	40	0.40	± 0.06	204.3	± 26.9	1.8	± 0.26	12.3	± 1.6	7.9
Ad	20	0.36	± 0.05	214.2	± 21.1	2.7	± 0.26	8.4	± 1	11.6
	30	0.37	± 0.04	222.4	± 20.5	2.2	± 0.30	10.6	± 1.1	12.9
	40	0.36	± 0.06	225.7	± 30.4	1.8	± 0.26	13.5	± 1.5	8.3
Ae	20	0.26	± 0.04	294.5	± 30.1	2.7	± 0.26	11.6	± 1.5	10.5
	30	0.29	± 0.03	284.1	± 21.9	2.2	± 0.30	13.6	± 1.4	12.8
	40	0.29	± 0.05	288.6	± 28.6	1.8	± 0.26	17.1	± 1.7	12

(a)

(b)

(c)
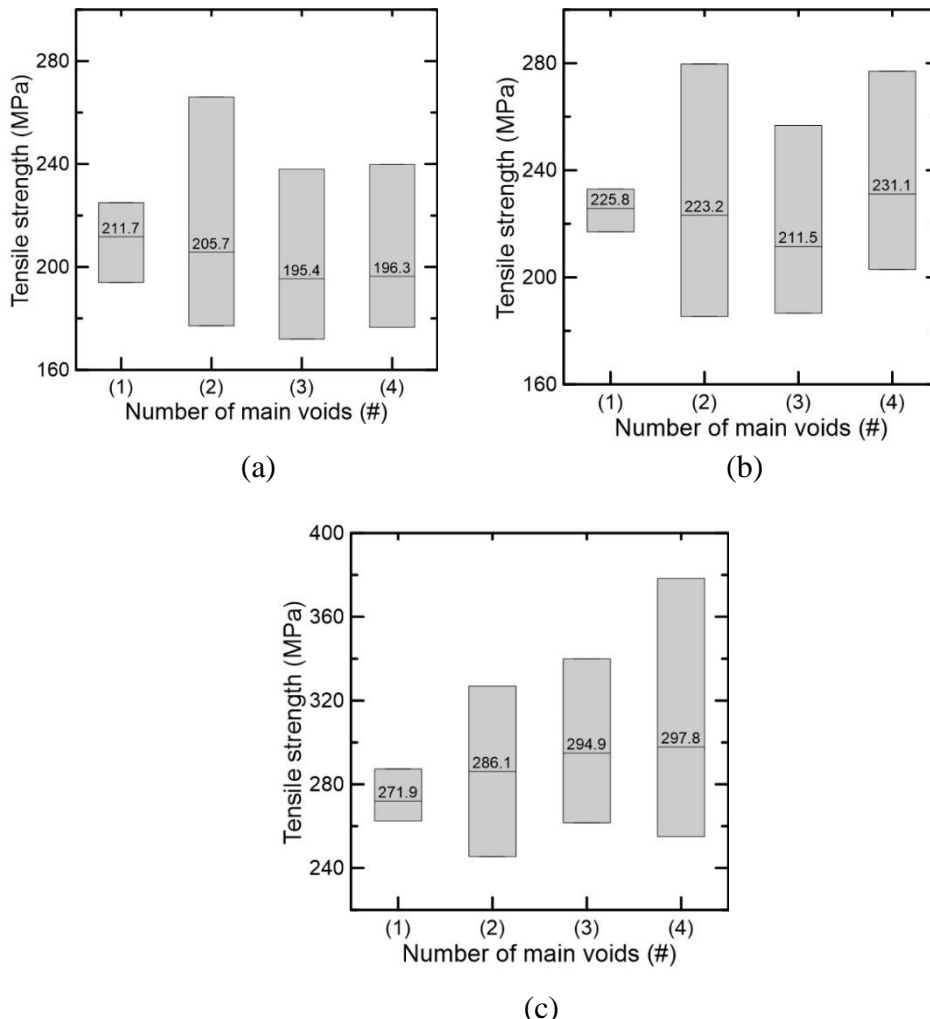
Fig. 9. The influence of major voids on the fiber tensile strength: (a) total area, (b) area without main voids, and (c) effective area void

The average tensile strength was not influenced by the gauge length, but the strain-to-failure of the fibers decreased with increasing gauge length. This behavior was related to the average size and distribution of flaws in the volume of the fiber, and was also observed in other vegetable fibers (Fidelis *et al.* 2013). This was traced back to the mean flaw size distribution, which did not change with gauge length. Once a crack formed at the largest flaw, how quickly the linkage between flaws occurred determined the strain values. The average tensile strength of the fibers did not vary when the number of main lumen increased (Fig. 9). The peach palm strength was a function of its diameter for all computed areas, as shown in Fig. 10.

(a)

(b)

(c)
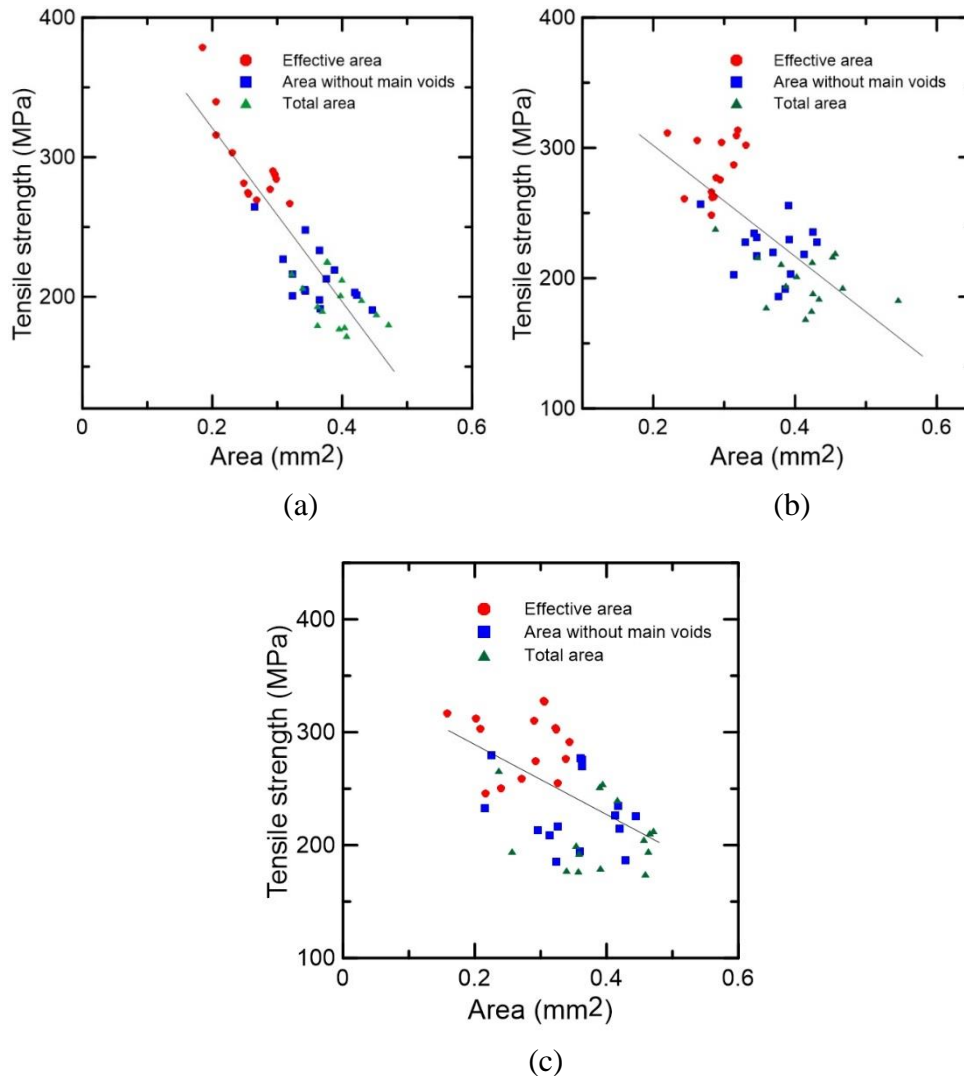
Fig. 10. The effect of the different areas on the fiber tensile strength: (a) fiber length of 20 mm, (b) fiber length of 30 mm, and (c) fiber length of 40 mm

Most works that have been based on a similar investigation to the one presented in this paper (Zhang *et al.* 2015; Trujillo *et al.* 2014; Hoyos *et al.* 2012; Rosa *et al.* 2010) did not correlate the fiber morphology with its tensile behavior. Since the vegetable fibers present a complex cellular structure, it is of great importance the computation of the area by image analysis in order to investigate the influence of the fiber microstructure with its

bioresources.com

tensile behavior. Also the use of a micro-force testing system and the calculation of the machine compliance results in precise values of fiber strength and elastic modulus.

The peach palm fibers varied in tensile strength, which is characteristic of natural fibers. This variability can be explained by the distribution of defects within the fiber or over the fiber surface. Weibull statistics was used to classify the fiber strength *versus* the relative probability of failure of the fibers in order to obtain a measure of variability in fiber strength (Silva *et al.* 2008). According to the Weibull analysis, the probability of survival for a fiber with a maximum stress, σ, is given by Eq. 3,

$$P(\sigma) = \exp\left[-\left(\frac{\sigma}{\sigma_0} \right)^m \right] \tag{3}$$

where m stands for the Weibull modulus, and σ (MPa) is the fiber resistance to a probability of survival defined as σ_0 (MPa).

(a)

(b)

(c)
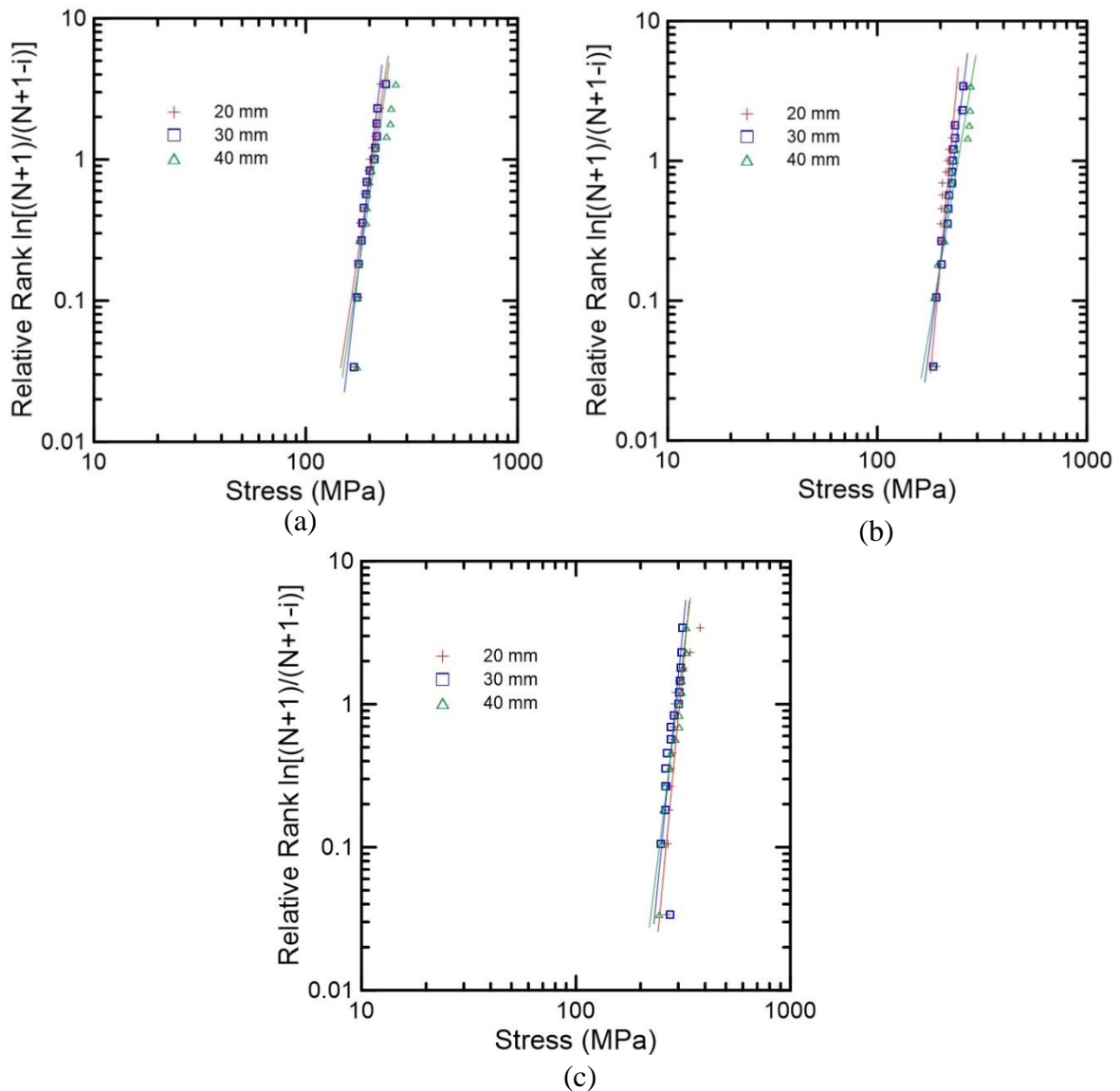
Fig. 11. The Weibull distribution for peach palm fiber for different gauge lengths according to: (a) the total area, (b) area without main voids, and (c) effective area void

(a)

(b)

(c)

(d)
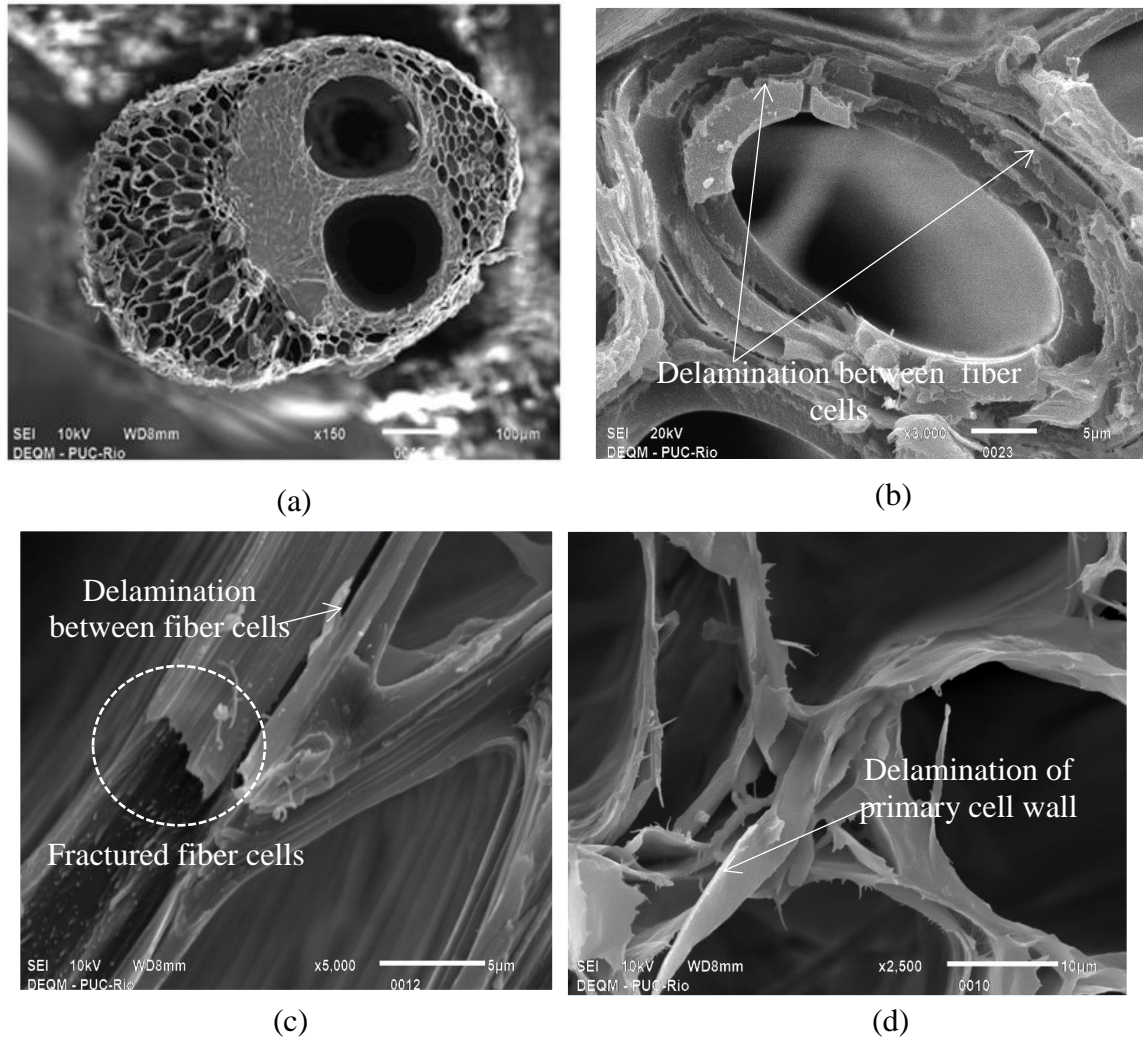
Fig. 12. Peach palm fiber failure modes: (a) general view of the fiber after the fracture, (b) delamination of the fiber walls, (c) fracture of the fiber cells and delamination between walls of the fiber cells, and (d) delamination of the primary wall

A greater *m* value results in a lower variability in the resistance value of *m*. The ranking of the resistance values is found using an estimator given by Eq. 4 (Silva *et al.* 2008),

$$P(\sigma)_i = 1 - \frac{i}{N+1} \tag{4}$$

where $P(\sigma)$ is the probability of survival corresponding to the resistance value of *i* (MPa), and *N* is the total number of fibers measured. Substituting Eq. 4 in Eq. 3, the following equation is obtained,

$$\ln\ln\left[\frac{N+1}{N+1-i}\right] = m\ln\left(\frac{\sigma}{\sigma_0}\right) \tag{5}$$

The slope of ln ln [(N + 1) / (N + 1 - *i*)] *versus* ln σ / σ₀ is called the Weibull modulus, *m*.

The Weibull modulus is a measure of variability in the strength of the fibers. The tensile strength of peach palm fibers had a low variability (Table 1). When *At* was used, the Weibull modulus varied between 7 and 12 (Fig. 11a). When taking into account *Ad*, *m* varied from 8 to 12 (Fig. 11b), and for *Ae*, the value of *m* varied between 10 and 12 (Fig. 11c).

Figure 12 shows the fracture surface of the peach palm fibers after the tensile tests. The fracture of the fibers occurred by three processes. The first was the delamination of the fiber cell walls (Fig. 12d), the second was the delamination between fiber cells (Fig. 12b, 12c), and the third was the fracture of the fiber cells (Fig. 12c). The delamination between fiber cells seemed to be a secondary damage process. This was different than what was observed for other natural fibers, like sisal. For sisal, the delamination between the fiber cells contributed to the change in the slope of the stress-strain curve. For the peach palm fiber, this non-linear behavior was not observed, probably because of a less severe delamination process of the fiber cells.

CONCLUSIONS

1. The TGA results showed that the fiber was thermally stable up to 280 °C. This is an important characteristic for cementitious composites that are submitted to elevated temperatures during their life cycle. Compared with other lignocellulosic fibers, the fiber also had a superior CI of 71%.

2. The fiber void content had a large influence on the fiber tensile strength and elastic modulus. As the fiber got closer to its effective area, both its tensile strength and its modulus of elasticity increased to 90 MPa and 4 GPa, respectively, due to a high porosity of the fiber.

3. The Weibull modulus decreased with increasing gauge length. This can be explained by the fact that the average size of flaws was independent of the reference length, but the number of flaws increased with increasing volume. Thus, while the medium size of flaws results in failure control, the number of flaws plays a more important role in controlling the strain-to-failure.

4. The mechanical tests coupled with the microstructural investigation showed that the number of main voids did not influence the fiber strength. Therefore, every fiber with morphology independent of the number of main lumens can be safely used for reinforcement in composites.

ACKNOWLEDGMENTS

REFERENCES CITED

Akil, H. M., Omar, M. F., Mazuki, A. A. M., Safiee, S., Ishak, Z. A. M., and Bakar, A. Abu (2011). "Kenaf fiber reinforced composites: A review," *Mater. Design* 32(8-9), 4107-4121. DOI: 10.1016/j.matdes.2011.4.008

ASTM C1557 (2014). "Standard test method for tensile strength and Young's modulus of fibers," ASTM International, West Conshohocken, PA, USA.

Baley, C. (2002). "Analysis of the flax fibres tensile behaviour and analysis of the tensile stiffness increase," *Compos. Part A-Applied S.* 33(7), 939-948. DOI: 10.1016/S1359-835X(02)00040-4

Belouadah, Z., Ati, A., and Rokbi, M. (2015). "Characterization of new natural cellulosic fiber from *Lygeum spartum* L.," *Carbohyd. Polym.* 134, 429-437. DOI: 10.1016/j.carbpol.2015.08.024

Bezazi, A., Belaadi, A., Bourchak, M., Scarpa, F., and Boba, K. (2014). "Novel extraction techniques, chemical and mechanical characterisation of *Agave americana* L. natural fibres," *Compos. Part B-Eng.* 66, 194-203. DOI: 101.1016/j.compositesb.2014.05.014

Binoj, J. S., Edwin Raj, R., Sreenivasan, V. S., and Rexin Thusnavis, G. (2016). "Morphological, physical, mechanical, chemical and thermal characterization of sustainable Indian areca fruit husk fibers (*Areca catechu* L.) as potential alternate for hazardous synthetic fibers," *Journal of Bionic Engineering* 13(1), 156-165.DOI: 10.1016/S1672-6529(14)60170-0

Brahim, S. B., and Cheikh, R. B. (2007). "Influence of fibre orientation and volume fraction on the tensile properties of unidirectional alfa-polyester composite," *Compos. Sci. Technol.* 67(1), 140-147. DOI: 10.1016/j.compscitech.2005.10.006

Carvalho, K. C. C., Mulinari, D. R., Voorwald, H. J. C., and Cioffi, M. O. H. (2010). "Chemical modification effect on the mechanical properties of hips/ coconut fiber composites," *BioResources* 5(2), 1143-1155. DOI: 10.15376/biores.5.2.1143-1155

Chakrabarty, J., Masudul Hassan, M., Khan, and Mubarak A. (2012). "Effect of surface treatment on betel nut (*Areca catechu*) fiber in polypropylene composite," *Journal of Polymers and the Environment* 20, 501-506. DOI 10.1007/s10924-011-0405-2

d'Almeida, J. R. M., Aquino, R. C. M. P., and Monteiro, S. N. (2006). "Tensile mechanical properties, morphological aspects and chemical characterization of piassava (*Attalea funifera*) fibers," *Compos. Part A-Applied S.* 37(9), 1473-1479. DOI: 10.1016/j.compositesa.2005.03.035

d'Almeida, J. R. M., d'Almeida, A. L. F. S., and Carvalho, L. H. d. (2008). "Mechanical, morphological, and structural characteristics of caroa (*Neoglaziovia variegata*) fibres," *Polym. Polym. Compos.* 16(9), 589-595.

d'Almeida, J. R. M., Mauricio, M. H. P., and Paciornik, S. (2012). "Evaluation of the cross-section of lignocellulosic fibers using digital microscopy and image analysis," *J. Compos. Mater.* DOI: 10.1177/0021998311435532.

De Rosa, I. M., Kenny, J. M., Maniruzzaman, M., Moniruzzaman, M., Monti, M., Puglia, D., Santulli, C., and Sarasini, F. (2011). "Effect of chemical treatments on the mechanical and thermal behaviour of okra (*Abelmoschus esculentus*) fibres," *Compos. Sci. Technol.* 71(2), 246-254. DOI: 10.1016/j.compscitech.2010.11.023

De Rosa, I. M., Kenny, J. M., Puglia, D., Santulli, C., and Sarasini, F. (2010). "Morphological, thermal and mechanical characterization of okra (*Abelmoschus*

esculentus) fibres as potential reinforcement in polymer composites," *Compos. Sci. Technol.* 70(1), 116-122. DOI: 10.1016/j.compscitech.2009.09.013

De Souza, N. C. R., and d'Almeida, J. R. M. (2014). "Tensile, thermal, morphological and structural characteristics of abaca (musa textiles) fibers," *Polymers from Renewable Resources* 5(2), 47-60.

Defoirdt, N., Biswas, S., Vriese, L. D., Tran, L. Q. N., Acker, J. V., Ahsan, Q., Gorbatikh, L., Vuure, A. V., and Verpoest, I. (2010). "Assessment of the tensile properties of coir, bamboo and jute fibre," *Compos. Part A-Applied S.* 41(5), 588-595. DOI: 10.1016/j.compositesa.2010.01.005

Dittenber, D. B., and GangaRao, H. V. S. (2012). "Critical review of recent publications on use of natural composites in infrastructure," *Compos. Part A-Applied S.* 43(8), 1419-1429. DOI: 10.1016/j.compositesa.2011.11.019

Ferreira, S. R., Silva, A. M. D., Souza Jr., F. G. D., Filho, R. D. T., and Andrade Silva, F. d. (2014). "Effect of polyaniline and H_2O_2 surface modification on the tensile behavior and chemical properties of coir fibers," *Journal of Biobased Materials and Bioenergy* 8(6), 578-586. DOI: 10.1116/jbmb.2014.1478

Fidelis, M. E. A., Pereira, T. V. C., Gomes, O. d. F. M., Silva, F. d. A., and Filho, R. D. T. (2013). "The effect of fiber morphology on the tensile strength of natural fibers," *Journal of Materials Research and Technology* 2(2), 149-157. DOI: 10.1016/j.jmrt.2013.02.003

Fiore, V., Scalici, T., and Valenza, A. (2014). "Characterization of a new natural fiber from *Arundo donax* L. as potential reinforcement of polymer composites," *Carbohyd. Polym.* 106, 77-83. DOI: 10.1016/j.carbpol.2014.02.016

George, J., Sreekala, M. S., and Thomas, S. (2001). "A review on interface modification and characterization," *Polym. Eng. Sci.* 41(9), 1471-1485. DOI: 10.1002/pen.10846

Hota, G., and Liang, R. (2011). "Advanced fiber reinforced polymer composites for sustainable civil infrastructures," in: *International Symposium on Innovation & Sustainability of Structures in Civil Engineering*, Xiamen University, Fujian, China.

Hoyos, C. G., Alvarez, V.A., Rojo, P. G., and Vázquez, A. (2012). "Fique fibers: Enhancement of the tensile strength of alkali treated fibers during tensile load application," *Fibers and Polymers* 13(5), 632-640. DOI 10.1007/s12221-012-0632-8

Jayaramudu, J., Guduri, B. R., and Varada Rajulu, A. (2010). "Characterization of new natural cellulosic fabric *Grewia tilifolia*," *Carbohyd. Polym.* 79(4), 847-851. DOI: 10.1016/j.carbpol.2009.10.046

Marinelli, A. L., Monteiro, M. R., Ambrósio, J. D., Branciforti, M. C., Kobayashi, M., and Nobre, A. D. (2008). "Desenvolvimento de compósitos poliméricos com fibras vegetais naturais da biodiversidade: Uma contribuição para a sustentabilidade amazônica," *Polímeros: Ciência e Tecnologia* 18(2), 92-99. DOI:10.1590/S0104-14282008000200005

Padmaraj, N. H., Vijay Kini, M., Raghuvir Pai, B., and Satish Shenoy, B. (2013). "Development of short areca fiber reinforced biodegradable composite material," *Procedia Engineering* 64, 966-972. DOI: 10.1016/j.proeng.2013.09.173

Porras, A., Maranon, A., and Ashcroft, I. A. (2015). "Characterization of a novel natural cellulose fabric from *Manicaria saccifera* palm as possible reinforcement of composite materials," *Compos. Part B-Eng.* 74, 66-73. DOI: 10.1016/j.compsitesb.2014.12.033

Prasad, A. V. R., and Rao, K. M. (2011). "Mechanical properties of natural fibre reinforced polyester composites: Jowar, sisal and bamboo," *Mater. Design* 32(8-9), 4658-4663. DOI: 10.1016/j.matdes.2011.03.015

Rong, M. Z., Zhang, M. Q., Liu, Y., Yang, G. C., and Zeng, H. M. (2001). "The effect of fiber treatment on the mechanical properties of unidirectional sisal-reinforced epoxy composites," *Compos. Sci. Technol.* 61(10), 1437-1447. DOI: 10.1016/S0266-3538(01)00046-X

Rosa, I. M. D., Kenny, J. M., Puglia D., Santull, C., and Sarasini F. (2010). "Tensile behavior of New Zealand flax (*Phormium tenax*) fibers," *Journal of Reinforced Plastics & Composites* 29(23), 3450-3454. DOI: 10.1177/0731684410372264

Santos, A. S., Farina, M. Z., Pezzin, A. P. T., and Silva, D. A. K. (2007). "The application of peach palm fibers as an alternative to fiber reinforced polyester composites," *J. Reinf. Plast. Comp.* 27(16-17), 1805-1816. DOI: 10.1177/0731684407082634

Sarikanat, M., Seki, Y., Sever, K., and Durmuşkahya, C. (2014). "Determination of properties of *Althaea officinalis* L. (marshmallow) fibres as a potential plant fibre in polymeric composite materials," *Compos. Part B-Eng.* 57, 180-186. DOI: 10.1016/j.compositesb.2013.09.041

Seki, Y., Sarikanat, M., Sever, K., and Durmuşkahya, C. (2013). "Extraction and properties of *Ferula communis* (chakshir) fibers as novel reinforcement for composites materials," *Compos. Part B-Eng.* 44(1), 517-523. DOI: 10.1016/j.compositesb.2012.03.013

Silva, F. d. A., Chawla, N., and Filho, R. D. d. T. (2008). "Tensile behavior of high performance natural (sisal) fibers," *Compos. Sci. Technol.* 68(15-16), 3438-3443. DOI: 10.1016/j.compscitech.2008.10.001

Srinivasa, C.V., Arifulla, A., Goutham, N., Santhosh, T., Jaeethendra, H. J., Ravikumar, R. B., Anil, S. G., Santhosh Kumar, D. G., and Ashish, J. (2011). "Static bending and impact behaviour of areca fibers composites," *Materials & Design* 32(4), 2469-2475. DOI:10.1016/j.matdes.2010.11.020

Spinacé, M. A. S., Lambert, C. S., Fermoselli, K. K. G., and Paoli, M.-A. D. (2009). "Characterization of lignocellulosic curaua fibres," *Carbohyd. Polym.* 77(1), 47-53. DOI: 10.1016/j.carbpol.2008.12.005

Sreenivasan, V. S., Somasundaram, S., Ravindran, D., Manikandan, V., and Narayanasamy, R. (2011). "Microstructural, physico-chemical and mechanical characterisation of *Sansevieria cylindrica* fibres – An exploratory investigation," *Mater. Design* 32(1), 453-461. DOI: 10.1016/j.matdes.2010.06.004

Temer, B. C., and d'Almeida, J. R. M. (2012). "Characterization of the tensile behavior of pejibaye (*Bactris gasipaes*) fibers," *Polymers from Renewable Resources* 3(2), 33-42.

Tomczak, F., Satyanarayana, K. G., and Sydenstricker, T. H. D. (2007). "Studies on lignocellulosic fibers of Brazil: Part III – Morphology and properties of Brazilian curauá fibers," *Compos. Part A-Applied S.* 38(10), 2227-2236. DOI: 10.1016/j.compositesa.2007.06.005

Trujillo, E., Moesen, M., Osorio, L., Van Vuure, A. W., Ivens, J., and Verpoest, I. (2014). "Bamboo fibres for reinforcement in composite materials: Strength Weibull analysis," Composites: Part A 61, 115-125. DOI: 10.1016/j.compositesa.2014.02.003

Yusriah, L., Sapuan, S. M., Zainudin, E. S., and Mariatti, M. (2014). "Characterization of physical, mechanical, thermal and morphological properties of agro-waste betel nut

(*Areca catechu*) husk fibre," *Journal of Cleaner Production* 72(1), 174-180. DOI:10.1016/j.jclepro.2014.02.025

Zhang, T., Guo, M., Cheng, L., and Li, X. (2015). "Investigations on the structure and properties of palm leaf sheath fiber," *Cellulose* 22, 1039-1051. DOI: 10.1007/s10570-015-0570-x